

*Citation for published version:*

Siddique, M, Farooq, R & Price, GJ 2014, 'Synergistic effects of combining ultrasound with the Fenton process in the degradation of Reactive Blue 19', *Ultrasonics Sonochemistry*, vol. 21, no. 3, pp. 1206-1212.  
<https://doi.org/10.1016/j.ultsonch.2013.12.016>

*DOI:*

[10.1016/j.ultsonch.2013.12.016](https://doi.org/10.1016/j.ultsonch.2013.12.016)

*Publication date:*

2014

*Document Version*

Peer reviewed version

[Link to publication](#)

*Publisher Rights*

Unspecified

NOTICE: this is the author's version of a work that was accepted for publication in *Ultrasonics Sonochemistry*. Changes resulting from the publishing process, such as peer review, editing, corrections, structural formatting, and other quality control mechanisms may not be reflected in this document. Changes may have been made to this work since it was submitted for publication. A definitive version was subsequently published in *Ultrasonics Sonochemistry*, 21(3), 1206-1212, May 2014.  
[10.1016/j.ultsonch.2013.12.016](https://doi.org/10.1016/j.ultsonch.2013.12.016)

**University of Bath**

## Alternative formats

If you require this document in an alternative format, please contact:  
[openaccess@bath.ac.uk](mailto:openaccess@bath.ac.uk)

**General rights**

Copyright and moral rights for the publications made accessible in the public portal are retained by the authors and/or other copyright owners and it is a condition of accessing publications that users recognise and abide by the legal requirements associated with these rights.

**Take down policy**

If you believe that this document breaches copyright please contact us providing details, and we will remove access to the work immediately and investigate your claim.

## Accepted Manuscript

Synergistic effects of combining ultrasound with the Fenton process in the degradation of Reactive Blue 19

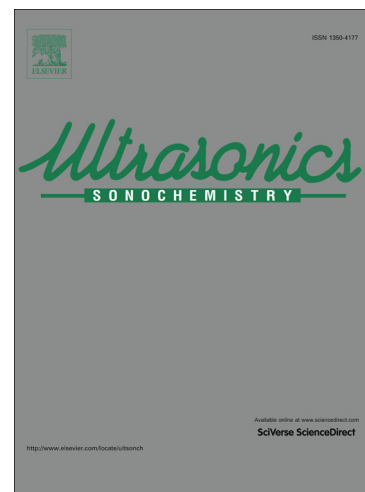
Maria Siddique, Robina Farooq, Gareth.J. Price

PII: S1350-4177(13)00323-4

DOI: <http://dx.doi.org/10.1016/j.ultsonch.2013.12.016>

Reference: ULTSON 2469

To appear in: *Ultrasonics Sonochemistry*



Please cite this article as: M. Siddique, R. Farooq, Gareth.J. Price, Synergistic effects of combining ultrasound with the Fenton process in the degradation of Reactive Blue 19, *Ultrasonics Sonochemistry* (2013), doi: <http://dx.doi.org/10.1016/j.ultsonch.2013.12.016>

This is a PDF file of an unedited manuscript that has been accepted for publication. As a service to our customers we are providing this early version of the manuscript. The manuscript will undergo copyediting, typesetting, and review of the resulting proof before it is published in its final form. Please note that during the production process errors may be discovered which could affect the content, and all legal disclaimers that apply to the journal pertain.

1 **Synergistic effects of combining ultrasound with the Fenton process in the**  
2 **degradation of Reactive Blue 19**

3 Maria Siddique<sup>a</sup>, Robina Farooq<sup>b</sup> Gareth. J. Price<sup>c</sup>

4 <sup>a</sup>Department of Environmental Sciences, COMSATS Institute of Information  
5 Technology, Abbottabad, Pakistan

6 <sup>b</sup>Department of Chemical Engineering, COMSATS Institute of Information  
7 Technology, Lahore, Pakistan

8 <sup>c</sup>Department of Chemistry, University of Bath, Bath BA2 7AY, UK

9  
10 Modifications to manuscript after review in red

11  
12 **Abstract**

13 The decoloration of reactive dye C.I. Reactive Blue 19 (RB 19) using combined  
14 ultrasound with the Fenton process has been investigated. The effect of varying the  
15 concentrations of hydrogen peroxide and iron sulphate, initial pH, ultrasonic power,  
16 initial dye concentration and dissolved gas on the decoloration and degradation  
17 efficiencies was measured. Calibration of the ultrasound systems was performed using  
18 calorimetric measurements and oxidative species monitoring using the Fricke dosimeter  
19 and degradations were carried out with a 20 kHz probe type transducer at 2, 4, 6, 8 W cm<sup>-2</sup>  
20 of acoustic intensity at 15, 25, 50, 75 mg L<sup>-1</sup> initial dye concentrations. First order rate  
21 kinetics was observed. It was found that while the degradation rate due to ultrasound  
22 alone was slow, sonication significantly accelerated the Fenton reaction. While the results  
23 were similar to those reported for other dyes, the effects occurred at lower concentrations.

24 The rate and extent of decoloration of RB 19 increased with rising hydrogen peroxide  
25 concentration, ultrasonic powers and iron sulphate concentration but decreased with  
26 increasing dye concentration. An optimum pH value of pH=3.5 was found. The rate of  
27 decoloration was higher when dissolved oxygen was present as compared with nitrogen  
28 and argon confirming the solution phase mechanism of the degradation.

29

30 **Keywords:** Dye degradation; ultrasound promoted fenton process; ultrasonic cavitation;  
31 dissolved gases; wastewater treatment

32

---

33 \*Corresponding author Email address: [maria@ciit.net.pk](mailto:maria@ciit.net.pk) (Maria Siddique), Tel: +92-  
34 992-383592, Fax: +92-992-383441

35

## 36 1. Introduction

37 A variety of chemically different dyes are used for various industrial applications  
38 such as textile dyeing, paper printing, leather, shoe polish, plastics, food coloring *etc.* A  
39 significant amount of these dyes enter the environment as wastewater [1]. There are more  
40 than 100,000 types of dyes commercially available and over  $7 \times 10^5$  tonnes of dyestuff  
41 are produced annually [2]. Reactive dyes are resistant to light, water and oxidizing agents  
42 and are therefore difficult to degrade once released into aquatic systems. The presence of  
43 very low concentrations of dyes in effluent can be highly visible and undesirable [3] on  
44 aesthetic grounds. Their presence disturbs aquatic communities present in ecosystem by  
45 obstructing light penetration and oxygen transfer into water bodies [4]. Moreover, they  
46 can be toxic and carcinogenic [5-7].

47 A number of treatment techniques have been developed to remove dyes from the  
48 wastewaters. Among these, advanced oxidation processes (AOPs) are effective in  
49 degrading many reactive dyes. The Fenton process is a homogeneous advanced oxidation  
50 process using an acidic mixture of hydrogen peroxide and ferrous ions [8, 9] to produce  
51 highly oxidative hydroxyl radicals which react with dissolved species, removing colour  
52 and lowering chemical oxygen demand. The  $\cdot\text{OH}$  radicals (Eq .1), attack the unsaturated  
53 dye molecule and the chromophore of the dye molecule is destroyed and decolorized [9].



55 The use of power ultrasound as an advanced oxidation process has been also  
56 employed in the degradation of textile dyes [8, 10]. This is also generally based on the  
57 formation of short-lived radical species generated in violent cavitation bubble collapses.  
58 These radical species can diffuse out of the bubble into the bulk fluid medium where they  
59 are able to react with solute molecules. A steady-state concentration of reactive radical  
60 species in the liquid phase can be maintained by continuous irradiation with ultrasound.  
61 Volatile solutes may evaporate into the bubble and be degraded by the harsh conditions  
62 generated during cavitation. Non-volatile organic compounds present in the liquid phase  
63 can undergo degradation mainly by reaction with powerful oxidizing agents such as  $\cdot\text{OH}$   
64 radicals produced [11]. The sonochemical enhancement of several AOPs has been  
65 reported. A number of studies have reported the use of ultrasound for the decoloration  
66 and degradation of textile dyes, but it has often been difficult to completely mineralize  
67 the dye stuff using ultrasound alone [12].

68 The combination of ultrasound with other advanced oxidation process is a  
69 convenient approach in degrading reactive dyes. There are a number of reports on the

70 combined use of ultrasound and Fenton process for the degradation of several textile dyes  
71 [8, 9, 13, 14]. While Guimaraes *et al.* [15] showed that oxidation of Reactive Blue 19 can  
72 be promoted by use of Fenton reagent and accelerated photochemically, the sono-Fenton  
73 process has not previously been applied to the degradation of this dye. Given its  
74 widespread use, [15, 16] the present study has focused on RB 19 dye to undergo  
75 treatment with combined Fenton and ultrasonic processes. The effect of the various  
76 experimental parameters including hydrogen peroxide and iron sulfate concentrations,  
77 pH, initial dye concentrations and dissolved gases on color removal were investigated.

78

## 79 **2. Experimental Procedure**

### 80 **2.1. Materials**

81 Reactive Blue 19 (RB 19) was purchased from Sigma Aldrich (UK) and was used  
82 as received; its structure is shown in Fig. 1.  $\text{FeSO}_4 \cdot 7\text{H}_2\text{O}$  (analytical grade) was obtained  
83 from BDH Laboratory Supplies (England). Hydrogen peroxide (analytical grade) 35%  
84 w/v,  $\text{H}_2\text{SO}_4$  and NaOH were obtained from Fisher Scientific (UK). All solutions were  
85 prepared with distilled water. Gases were obtained from BOC and were used without  
86 further purification.

### 87 **2.2. Procedure**

88 A stock solution of RB 19, prepared by dissolving 1 g of dye in 1 L of distilled  
89 water, was diluted to give initial concentrations for each experiment of  $25 \text{ mg L}^{-1}$  ( $4 \times 10^{-5}$   
90  $\text{ mol L}^{-1}$ ). Sulphuric acid and sodium hydroxide were used to adjust the pH of the dye  
91 solution. 100 mL volumes from the stock solution were placed in the glass reactor, and  
92 the appropriate amount of hydrogen peroxide and iron sulphate added to the solution. The

93 glass reactor was equipped with a water circulating jacket for maintaining reaction  
94 temperature to  $\pm 1$  °C. Sonication was performed with a Sonic processor L500-20  
95 ultrasonic generator (20 kHz, 200W, Sonic Systems) equipped with titanium probe  
96 transducer (23820T). The tip of the horn was 1 cm in diameter and was placed 1.5 cm  
97 into the liquid layer (Fig. 2). At 5 min time intervals, samples were taken from the reactor  
98 and analyzed by UV/visible spectrophotometry (Agilent 8453) using detection  
99 wavelengths of 256 and 594 nm. Each experiment was performed in duplicate. Sonication  
100 was conducted in the presence of air with no added gas except when the effect of  
101 dissolved gas was being investigated. In these experiments, the initial solution was  
102 vigorously purged with Argon, O<sub>2</sub> or N<sub>2</sub> for 20 min prior to ultrasonic irradiation and a  
103 gas flow of *approx.* 1 ml min<sup>-1</sup> was maintained throughout the experiment.

104 The percentage (%) decolorization was found from equation (2)

$$105 \text{ Dye \% decolorization} = (1 - C_t / C_0) \times 100 \quad (2)$$

106 where  $C_t$  and  $C_0$  are the concentrations (mg L<sup>-1</sup>) of dye at reaction time  $t$  and prior to  
107 sonication respectively [12]. The change in concentration in the solution was calculated  
108 from the Beer-Lambert law [13].

$$109 A = l \varepsilon C \quad (3)$$

110 where  $A$  is the absorbance,  $l$  is the path length (cm),  $\varepsilon$  is the molar extinction coefficient  
111 (L mol<sup>-1</sup> cm<sup>-1</sup>) and  $C$  is the dye concentration (mol L<sup>-1</sup>).

### 112 **2.3. Instrumentation**

113 The samples were collected at different time intervals and the degradation  
114 products were identified using Liquid chromatography/mass spectrometry (LC/MS). The  
115 mass spectrometry was performed using a microTOF electrospray time of flight (ESI-

116 TOF) mass spectrometer (Bruker Daltonik GmbH, Bremen, Germany) coupled to an  
117 Agilent 1200 LC system (Agilent Technologies, Waldbronn, Germany). The LC was  
118 equipped with a Phenomenex Luna 5 $\mu$  C18 (2) column with stationary phase mesh size of  
119 100 Å and dimensions (50 mm x 2 mm), connected directly to the MS. The other  
120 experimental conditions were: nitrogen supplied at a pressure of 1 bar as a nebulising gas  
121 and also used as the drying gas, with the flow rate of 8 L min<sup>-1</sup> at a temperature of 200°C,  
122 water/acetonitrile was employed as mobile phase with a flow rate of 0.4 mL min<sup>-1</sup>,  
123 sample volume 1  $\mu$ l, injection temperature 25 °C. For the detection of positive/negative  
124 ions a capillary voltage of -4000 V/ +4000 V was used.

#### 125 **2.4. Effects of acoustic intensity and sonolysis**

126 The acoustic power dissipated by the horn into the solution in the reactor was  
127 measured using the usual calorimetric method [17] employing a digital thermometer that  
128 recorded the solution temperature every 5 min, over a 30 min interval. The overall power  
129 input was estimated according to Eq. (4).

$$130 \text{ Energy input, } q = mc \, dT/dt \quad (4)$$

131 where  $m$  is the mass of water;  $c$  is the heat capacity of water and  $dT/dt$  is the temperature  
132 gradient over time. The acoustic intensity (W cm<sup>-2</sup>) was determined by dividing the  
133 power input ( $q$ ) by the horn surface area ( $A$ ).

#### 134 **2.5. Oxidizing species determination**

135 The homogeneous system used to monitor radical activity was Fricke dosimetry,  
136 in which iron II ions are oxidized (Eq. 5) by sonochemically generated species to iron III  
137 [17]. When the ultrasound is irradiated into a Fricke solution Fe<sup>+2</sup> ions in the solution are  
138 oxidized to Fe<sup>+3</sup> ions as follows:





140 The Fricke solution was prepared with 0.001 M ( $\text{FeSO}_4 \cdot 7\text{H}_2\text{O}$ ) and 0.005 M ( $\text{H}_2\text{SO}_4$ ).

141 The concentration of  $\text{Fe}^{+3}$  formed during irradiation was measured by a UV/Visible  
142 spectrophotometry at wavelength of 304 nm.

143

### 144 **3. Results and Discussion**

#### 145 *3.1. Decolorization of RB 19 in different systems*

146 Experiments were performed using  $\text{H}_2\text{O}_2$  alone,  $\text{FeSO}_4$  alone,  $\text{H}_2\text{O}_2 / \text{FeSO}_4$  and  
147 ultrasound combined with  $\text{H}_2\text{O}_2 / \text{FeSO}_4$  to observe independently the effects of different  
148 parameters on RB 19 decoloration. Color removal over treatment times of 30 min was  
149 less than 5% when  $\text{H}_2\text{O}_2$  alone,  $\text{FeSO}_4$  alone or ultrasound alone was used. Due to the  
150 non-volatile and hydrophilic nature of reactive dyes, decoloration would be expected to  
151 occur mainly in the bulk solution by radical reaction rather than inside the bubbles by  
152 pyrolytic reaction. At a frequency of 20 kHz, the concentration of hydroxyl radicals  
153 produced in the bulk solution by ultrasound alone was too low to affect the dye  
154 decoloration. Also the limited oxidizing power of hydrogen peroxide ( $E^0 = 1.78 \text{ V}$ )  
155 means that no color removal could be achieved by hydrogen peroxide alone. However, as  
156 shown in Fig. 3, reduction in color was observed when the combined  $\text{H}_2\text{O}_2 / \text{FeSO}_4$   
157 system was used, resulting from the generation of hydroxyl ( $\cdot\text{OH}$ ) radicals in the solution  
158 as Equation (1). This contrasts with a related dye (CI Reactive Black 8) on which Zhang  
159 and co-workers [13] showed ultrasound had no significant effect on decolourisation by  
160 Fenton reagent although other systems have demonstrated a beneficial effect [8, 14, 15]  
161 similar to that seen here.

162 Non-volatile organic compounds present in the liquid phase undergo degradation  
163 mainly by reaction with these  $\cdot\text{OH}$  radicals ( $E^0 = 2.8 \text{ V}$ ). Further, the combined  
164 ultrasound/ $\text{H}_2\text{O}_2$  / $\text{FeSO}_4$  system led to enhanced color removal, indicating an accelerating  
165 effect due to cavitation [8]. The highest amount of decoloration of about 78% was found  
166 in the coupled ultrasound and  $\text{H}_2\text{O}_2$  / $\text{FeSO}_4$  system after 30 min of treatment, while only  
167 50% of decolorization was obtained with  $\text{H}_2\text{O}_2$  / $\text{FeSO}_4$  in the absence of ultrasound. A  
168 detailed comparison with other published systems is complicated by the use of different  
169 conditions but these results indicate that using ultrasound can enhance the action of the  
170  $\text{H}_2\text{O}_2$  / $\text{FeSO}_4$  system so that each experimental parameter was studied to determine the  
171 origin of the effects.

### 172 **3.2. Effect of hydrogen peroxide concentration on RB 19 dye decolorization**

173 The decoloration of RB 19 at different concentrations of hydrogen peroxide was  
174 investigated (Fig. 4(a)) with a  $\text{FeSO}_4$  concentration of  $3 \text{ mg L}^{-1}$ , pH of 3.5 and ultrasonic  
175 intensity of  $8 \text{ W cm}^{-2}$ . As with previous studies using both homogeneous [13, 15] and  
176 heterogeneous [14] sono-Fenton reactions, it was found that the rate of decoloration  
177 increased with higher hydrogen peroxide concentration. It is notable that the  
178 concentrations of hydrogen peroxide used here were lower than that used in previously  
179 published studies and indicates that ultrasound may be applied at lower concentrations  
180 than previously suggested and so useful in minimizing the amount of reagent necessary  
181 for dye treatment. When hydrogen peroxide concentration was 0.05 mM the decoloration  
182 efficiency was *approx.* 55 % after 30 min of reaction time.

183 When the hydrogen peroxide concentration was increased to 0.5 mM the  
184 decoloration efficiency increased due to the higher concentrations of generated hydroxyl

185 radicals [8, 9]. The decolorization rate increased as the H<sub>2</sub>O<sub>2</sub> concentration increased  
186 from 0.05 mM to 0.5 mM although further increase in concentration did not lead to the  
187 further increase in decoloration. This can be explained since only a comparatively small  
188 amount of additional hydrogen peroxide decomposed to generate hydroxyl radicals and  
189 the undecomposed hydrogen peroxide may act as a scavenger for ·OH resulting in the  
190 generation of hydroperoxy radicals (Eq. 6) that are less reactive than the hydroxyl  
191 radicals. At these higher H<sub>2</sub>O<sub>2</sub> concentrations, hydroxyl radicals react with the peroxide  
192 in preference to the RB19 so the degradation rate is reduced.



194 Fig. 4(b) illustrates the kinetics of RB 19 decoloration and demonstrates that it fits  
195 a first order kinetic model as in Eq. (7).

$$196 \quad \ln (C_t/C_0) = -kt \quad (7)$$

197 where  $k$  is the first order rate constant (min<sup>-1</sup>) and  $t$  is reaction time in min. The  
198 relationship between hydrogen peroxide concentration and first order rate constant is  
199 shown in Fig. 4(c).

### 200 **3.3. The effect of initial pH on the RB 19 dye decolorization**

201 The pH values investigated were 2.5, 3.5, 4.5, 5.5 at a fixed FeSO<sub>4</sub> concentration  
202 of 3 mg L<sup>-1</sup>, H<sub>2</sub>O<sub>2</sub> concentration of 0.5 mM and ultrasonic intensity of 8 W cm<sup>-2</sup>. It can be  
203 seen from Fig. 5(a) that the decoloration rate increased with decreasing pH, reaching a  
204 maximum at pH 3.5 after which the rate decreased. Zhang *et al.* [8, 13] reported that the  
205 rate of decolouration was relatively insensitive to pH below pH=6 although the reduction  
206 of chemical oxygen demand was maximized at pH=3. Similar results on other dyes have  
207 been reported [10]. The pH is an important parameter in Fenton reactions and it has often

208 been reported that that the optimum pH is around pH = 3 is usually optimum for Fenton  
209 oxidations [18, 19, 20]. Accordingly, the first order rate constant decreases linearly with  
210 the increase of pH (> 3.5) as shown in Fig. 5(b). This variation of reaction rate with pH  
211 arises from a complex mixture of factors. At low pH (< 2.5), the high concentration of H<sup>+</sup>  
212 ions in solution dominates the reaction with ·OH (Eq. 8) [18].



214 Under these conditions, the rate of production of hydroxyl radicals is relatively  
215 slow since iron mainly exists as [Fe(H<sub>2</sub>O)<sub>2</sub>]<sup>+2</sup>. Iron is present in solution in catalytic  
216 amounts and a further limitation on the rate of ·OH production is the slow regeneration of  
217 Fe<sup>+2</sup> after reaction (1). [18].

218 These effects are less important as the pH rises and so the rate and extent of  
219 decolouration rises. However, above pH = 4, other effects come into play which reduce  
220 the rate [19-21]. The concentration of Fe<sup>+2</sup> in solution is reduced since Fe<sup>+3</sup> species are  
221 more stable in solution. Solid oxyhydroxides such as Fe(OH)<sub>3</sub> can also precipitate. Thus,  
222 lower concentrations of ·OH are generated and decolouration is less effective. These  
223 effects combine to give an optimum value of pH = 3.5 in this work as reported previously  
224 with other dyes.

#### 225 ***3.4. The effect of iron sulphate concentration on the RB 19 dye decolorization***

226 The effect of iron sulphate concentration on RB 19 dye decoloration was  
227 investigated with H<sub>2</sub>O<sub>2</sub> concentration fixed at 0.5 mM, pH value at 3.5 and ultrasonic  
228 intensity of 8 W cm<sup>-2</sup>. It was observed that the degradation of RB 19 increased with  
229 increasing Fe<sup>+2</sup> concentrations in solution (Fig. 6(a)) although the decoloration rate  
230 decreased when the iron sulphate concentration was above 3 mg L<sup>-1</sup>. High concentrations

231 of iron sulphate would produce too many ferrous ions in solution, resulting in scavenging  
232 of the  $\cdot\text{OH}$  radicals according to reaction (9) [9, 18] in preference to reaction with the  
233 dye.



235 The relationship between iron sulphate concentration loading and first order rate  
236 constant is shown in Fig. 6(b) and indicates that the rate constant increases linearly with  
237 the increase of iron loading. It should be noted that the concentration of  $\text{Fe}^{+2}$  used here is  
238 lower than that used in other studies although where comparison is possible, the  
239 degradation rate does increase with rising iron concentration under comparable  
240 conditions in published studies.

### 241 **3.5. Decay of UV/Visible absorption spectra**

242 The change in UV/Visible absorption spectra for RB 19 decoloration as a function  
243 of time was recorded (Fig. 7), using a  $\text{H}_2\text{O}_2$  concentration of 0.5 mM,  $\text{FeSO}_4$   
244 concentration of  $3 \text{ mg L}^{-1}$ , pH 3.5 and ultrasonic intensity of  $8 \text{ W cm}^{-2}$ . As can be seen  
245 from the spectra, before the oxidation, the absorption spectrum of RB 19 was  
246 characterized by two main bands, in UV region (256 nm) and in visible region (594 nm).  
247 The disappearance of the visible band was likely due to the fragmentation of  
248 anthraquinone bond by oxidation and change in absorbance in UV region was considered  
249 as evidence of aromatic fragment degradation in dye molecule and its degradation  
250 products [8]. Initial radical attack occurs at the aromatic substituent on the anthraquinone  
251 ring and at the carbonyl groups [22].

252

253

### 254 **3.6. The effect of initial dye concentration on RB 19 decolorization**

255 Fig. 8(a) illustrates the decoloration of RB 19 at different initial dye  
256 concentrations when  $\text{H}_2\text{O}_2$  concentration is 0.5 mM,  $\text{FeSO}_4$  concentration is 3 mg  $\text{L}^{-1}$ , pH  
257 value is 3.5 and ultrasonic intensity of 8  $\text{W cm}^{-2}$ . It can be seen that higher initial dye  
258 concentrations led to decreased decolorization rates. This may be due to insufficient  
259 hydroxyl radical concentration to react with higher amounts of dye in solution. A  
260 concentration of 75 mg  $\text{L}^{-1}$  corresponds to 0.12 mmol  $\text{L}^{-1}$  which is well in excess of the  
261 expected generation of  $\cdot\text{OH}$ . Fig. 8(b) shows that the first order rate constant decreases  
262 with the increase of initial dye concentration. This behavior is typical of such  
263 sonochemical reactions.

264 A kinetic study using combined ultrasound and Fenton degradation processes was  
265 undertaken by measuring the rate constant ( $k$ ) for first, second and third order reactions.  
266 The values confirmed that the order of reaction within the current experimental  
267 conditions was first order as shown in Fig. 8(c) at different initial concentrations [23].  
268 The correlation between  $\ln(C_t/C_0)$  and irradiation time was linear (Fig. 8(c), the slopes  
269 giving the apparent rate constant ( $k$ ). The regression coefficient,  $R^2$ , values ranged from  
270 0.99 to 0.95, confirming that combined ultrasound and Fenton degradation process of RB  
271 19 followed the first order reaction kinetics.

### 272 **3.7. The effect of dissolved gases on RB 19 decolorization**

273 Several authors have showed the dependence on the saturating gas of the  
274 sonochemical treatment of organics in water [24, 25] although studies on dye systems are  
275 rare. Zhang *et al.* showed [8] little difference in the degradation of CI Acid Orange 7  
276 under nitrogen or oxygen. The nature of dissolved gas is an important parameter that

277 affects the sonochemical processes since it acts as nucleation sites for cavitation and also  
 278 influences the conditions such as final temperature achieved inside a collapsing cavitation  
 279 bubble [26]. Monatomic gases, with higher ratios of specific heat capacities,  $\gamma$ , such as  
 280 argon, promote increased temperature of collapse and hence higher levels of pyrolysis of  
 281 substances inside the cavitation bubbles. The physical properties, such as specific heat  
 282 ratio, of oxygen and nitrogen are similar and so similar temperatures are generated inside  
 283 collapsing bubbles. Any differences here are due to chemical effects. Thus, the gas  
 284 present in the solution plays a determinant role in the implosion conditions of the bubble  
 285 of cavitation and in the formation of radicals during the ultrasonic process.

286 Degradation of RB 19 was carried out under argon, nitrogen and oxygen with a  
 287  $\text{H}_2\text{O}_2$  concentration of 0.5 mM,  $\text{FeSO}_4$  concentration of  $3 \text{ mg L}^{-1}$ , pH 3.5 and ultrasonic  
 288 intensity of  $8 \text{ W cm}^{-2}$ . The results showed that the dye decoloration was enhanced when  
 289 dissolved oxygen is present as compared with nitrogen or argon (Fig. 9). The lowest  
 290 degradation rate was measured under argon. In the presence of argon, the generation of  
 291  $\cdot\text{OH}$  is due only to the decomposition of vapor water (Eq. (10)). Evidence for this is the  
 292 generation of  $\text{H}_2\text{O}_2$  under argon saturation compared with oxygen as dissolved gas [26].



294 Under oxygen atmosphere the degradation rates were higher as compared to argon and  
 295 nitrogen, since oxygen promotes the formation of  $\cdot\text{OH}$  radicals as in Eq. (12).



298 These results are consistent with the reaction of RB 19 with hydroxyl radicals in solution  
299 rather than through pyrolysis. If pyrolysis played a significant part in the degradation, a  
300 faster rate under argon would be expected and this is not seen.

### 301 **3.8. Effect of ultrasonic powers on RB 19 decolorization**

302 The effect of ultrasonic power settings are shown in Fig. 10 (a) with optimized  
303 conditions of other parameters. It can be seen that increase in ultrasonic intensities (0-8  
304 W cm<sup>-2</sup>) increases the dye decoloration rate. This has commonly been reported in  
305 sonochemical systems. The increase in ultrasonic powers would increase the mixing  
306 intensity due to turbulence generated by cavitation bubble collapse as well as micro  
307 jetting [8] in addition to yielding higher numbers of cavitation bubbles [17] and hence  
308 higher yields of hydroxyl radicals. Fig. 10 (b) shows that the first order rate constant  
309 increase with the increase of ultrasonic power settings.

310 By comparing the rate constant values of ultrasonic power settings with rate  
311 constant values of Fricke dosimetry, it was found that in combined ultrasound and Fenton  
312 process the production of ·OH radicals were almost 10 times more as compared to the  
313 ·OH radicals produced by alone ultrasound process (Table 1) in Fricke dosimetry.

### 314 **3.9. RB 19 degradation studies**

315 Attempts to identify the intermediates/end products after the treatment of RB 19  
316 were made using LC/MS. Samples at different time intervals were collected during the  
317 combined ultrasound and Fenton process when initial RB 19 concentration was 200 mg  
318 L<sup>-1</sup>, H<sub>2</sub>O<sub>2</sub> concentration was 0.5 mM, FeSO<sub>4</sub> concentration was 3 mg L<sup>-1</sup>, pH was 3.5 and  
319 ultrasonic intensities of 8 W cm<sup>-2</sup>. From the results of this oxidation process, it can be  
320 expected that the 5 min treatment resulted in the disappearance of dye molecule with



321 decreased peak areas of dye residues. The initial LC/MS results could not assist to  
322 propose the degradation mechanism of dye therefore; further analysis will be required to  
323 determine the low molecular weight compounds.

#### 324 **4. Conclusions**

325 This study showed the first results on the effect of combined ultrasound and  
326 Fenton's process on RB 19 dye removal. In general they demonstrate similar effects to  
327 other dyes that have been subjected to the process although there are some differences. In  
328 particular, significant decolourisation was detected at lower concentrations of iron and  
329 peroxide than comparable studies on other dyes showing that the use of ultrasound can  
330 save the cost and potential side effects of reagent use. Unlike some dye systems, a small  
331 amount of degradation was detected using ultrasound alone although this was too slow to  
332 be applied in practice. Using ultrasound accelerates the Fenton reaction by accelerating  
333 the production of hydroxyl radicals. The decoloration of RB 19 dye was increased with  
334 the increase of hydrogen peroxide concentration, ultrasonic power and iron sulphate  
335 concentration but decreased by increasing the initial dye concentration. The process was  
336 optimized at  $\text{pH} = 3.5$ . The decoloration of RB 19 follows first order rate constant. The  
337 primary mechanism of reaction with hydroxyl radicals in solution rather than by pyrolysis  
338 was confirmed since the rate of decoloration was higher when dissolved oxygen was  
339 present as compared with nitrogen or argon.

#### 340 **Acknowledgements**

341 The study was financially supported by Higher Education Commission of  
342 Pakistan under the "International Research Support Initiative Programme, (IRSIP)".

343

344 **References**

- 345 [1]. G. McKay, Waste colour removal from textile effluents, *Am. Dyestuff Reporter*.  
346 68 (1979) 29.
- 347 [2]. V. Jaikumar, V. Ramamurthi, Effect of Biosorption Parameters Kinetics Isotherm  
348 and Thermodynamics for Acid Green Dye Biosorption from Aqueous Solution by  
349 Brewery Waste, *Int. J .Chem.* 1 (2009) 2.
- 350 [3]. S. Kim, C. Park, T.H. Kim, J. Lee, S.W. Kim, COD reduction and decolorization  
351 of textile effluent using a combined process, *J. Biosci. Bioeng.* 95 (2003) 102.
- 352 [4]. W.G. Kuo, Decolorizing dye wastewater with Fenton's reagent, *Water Res.* 26  
353 (1992) 881.
- 354 [5]. J. S. Bae, H. S. Freeman, Aquatic toxicity evaluation of new direct dyes to the  
355 *Daphnia*, *Dye Pigment.* 73 (2007) 81.
- 356 [6]. R.D. Combes, R.B. Havelandsmith, A review of the genotoxicity of food, drug  
357 and cosmetic colors and other azo, triphenyl methane and xanthene dyes,  
358 *Mutation. Res.* 98 (1982) 101.
- 359 [7]. H.S. Rai, M.S. Bhattacharyya, J. Singh, T.K. Bansal, P. Vats, U.C. Banerjee,  
360 Removal of dyes from the effluent of Textile and dye stuff manufacturing  
361 Industry: A review of emerging techniques with reference to biological treatment,  
362 *Crit. Rev. Env. Sci. Technol.* 35 (2005) 219.
- 363 [8]. H. Zhang, J. Zhang, C. Zhang, F. Liu, D. Zhang, Degradation of C.I. Acid Orange  
364 7 by the advanced Fenton process in combination with ultrasonic irradiation,  
365 *Ultrason. Sonochem.* 16 (2009) 325.

- 366 [9]. F. Emami, A.R. Tehrani-Bagha, K. Gharanjig, F.M. Menger, Kinetic study of the  
367 factors controlling Fenton-promoted destruction of a non-biodegradable dye,  
368 Desalination. 257 (2010) 124.
- 369 [10]. C. Ozdemir, M.K. Oden, S. Sahinkaya, E. Kalipc, Color Removal from Synthetic  
370 Textile Wastewater by Sono-Fenton Process, Clean - Soil, Air, Water. 39 (2011)  
371 60.
- 372 [11]. E.A. Mamdouh, R.B. Peter, A study investigating the sonoelectrochemical  
373 degradation of an organic compound employing Fenton's reagent, Phys. Chem.  
374 Chem. Phys. 4 (2002) 5340.
- 375 [12]. J.P. Lorimer, T.J. Mason, M. Plattes, S.S. Phull, D.J. Walton, Degradation of dye  
376 effluent, Pure Appl. Chem. 73 (2001) 1957.
- 377 [13]. H. Zhang, Y. Zhang and D. Zhang, Decolorization and mineralization of CI  
378 Reactive Black 8 by the Fenton and ultrasound/Fenton methods, Color. Technol.  
379 123 (2007) 101.
- 380 [14]. H. Zhang, H. Fu, D. Zhang, Degradation of C.I. Acid Orange 7 by ultrasound  
381 enhanced heterogeneous Fenton-like process, J. Hazard. Mater. 172 (2009) 654.
- 382 [15]. J.R. Guimaraes, M.G. Maniero, R.N. de Araújo A comparative study on the  
383 degradation of RB-19 dye in an aqueous medium by advanced oxidation  
384 processes, J. Environ. Manage. 110 (2012) 33.
- 385 [16]. S. Enes, M. E. Edecan, An optimization study using response surface methods on  
386 the decolorization of Reactive Blue 19 from aqueous solution by ultrasound,  
387 Ultrason. Sonochem. 15 (2008) 530.

- 388 [17]. G.J. Price, E.J. Lenz, The use of dosimeters to measure radical production in  
389 aqueous sonochemical systems, *Ultrasonics*. 31 (1993) 451.
- 390 [18]. G. E. Ustün, S.K. Solmaz, T. Morsünbül, H.S. Azak, Advanced oxidation and  
391 mineralization of 3-indole butyric acid (IBA) by Fenton and Fenton-like  
392 processes, *J. Hazard Mater.* 180 (2010) 508.
- 393 [19]. C. Duesterberg, S. Mylon, D. Waite pH Effects on Iron-Catalyzed Oxidation  
394 using Fenton's Reagent, *Environ. Sci. Technol.* 42 (2008) 8522.
- 395 [20]. P.R. Gogate, A.B. Pandit A review of imperative technologies for wastewater  
396 treatment I: oxidation technologies at ambient conditions, *Adv Environ Res.* 8  
397 (2004) 501.
- 398 [21]. S. Wang, A comparative study of Fenton and Fenton-like reaction kinetics in  
399 decolourisation of wastewater, *Dyes Pigm.* 76 (2008) 714.
- 400 [22]. M. Siddique, R Farooq, Z. M. Khan, Z. Khan, S. F. Shaukat, Enhanced  
401 decomposition of reactive blue 19 dye in ultrasound assisted electrochemical  
402 reactor *Ultrason. Sonochem.* 18 (2012) 190.
- 403 [23]. P.C. Fung, K.M. Sin, S.M. Tsui, Decolorization and degradation, kinetics of  
404 reactive dye wastewater by UV/ultrasonic / peroxide system, *J. Soc. Dyers.*  
405 *Colour.* 116 (2000) 170.
- 406 [24]. F. Mendez-Arriagad, R.A. Torres-Palmaa, C. Petriera, S. Esplugasd, J. Gimenezd,  
407 C. Pulgarinc, Ultrasonic treatment of water contaminated with ibuprofen, *Water*  
408 *Res.* 42 (2008) 4243.

- 409 [25]. R. Torres, C. Petrier, E. Combet, M. Carrier, C. Pulgarin, Ultrasonic cavitation  
410 applied to the treatment of bisphenol A. Effect of sonochemical parameters and  
411 analysis of BPA byproducts, *Ultrason. Sonochem.* 15 (2008) 605.
- 412 [26]. K. Yasui, T. Tuziuti, T. Kozuka, A. Towata, Y. Iida, Relationship between the  
413 bubble temperature and main oxidant created inside an air bubble under  
414 ultrasound, *J. Chem. Phys.* 127 (2007) 154502.
- 415

ACCEPTED MANUSCRIPT

**Figure Captions**

Fig. 1. Structure of RB 19 dye

Fig. 2. Experimental setup

Fig. 3. Decolorization of RB 19 by with/without H<sub>2</sub>O<sub>2</sub>, FeSO<sub>4</sub> by sonolysis (C<sub>0</sub>= 25 mg L<sup>-1</sup>, H<sub>2</sub>O<sub>2</sub> conc. 0.5 mM, FeSO<sub>4</sub> conc. 3 mg L<sup>-1</sup>, pH 3.5, US power =8 W cm<sup>-2</sup>)

Fig. 4 (a). The effect of hydrogen peroxide conc. on the decolorization of RB 19 (C<sub>0</sub>= 25 mg L<sup>-1</sup>, FeSO<sub>4</sub> conc. 3 mg L<sup>-1</sup>, pH 3.5, US power =8 W cm<sup>-2</sup>)

Fig. 4 (b). First order kinetic plot of RB 19 decoloration by different hydrogen peroxide conc. (C<sub>0</sub>= 25 mg L<sup>-1</sup>, FeSO<sub>4</sub> conc. 3 mg L<sup>-1</sup>, pH 3.5, US power = 8 W cm<sup>-2</sup>)

Fig. 4 (c). The effect of hydrogen peroxide concentration on the rate constant

Fig. 5 (a). The effect of pH on the decolorization of RB 19 (C<sub>0</sub>= 25 mg L<sup>-1</sup>, FeSO<sub>4</sub> conc. 3 mg L<sup>-1</sup>, H<sub>2</sub>O<sub>2</sub> conc. 0.5 mM, US power = 8 W cm<sup>-2</sup>)

Fig. 5 (b). The effect of different pH on the rate constant

Fig. 6 (a). The effect of iron sulphate addition on the decolorization of RB 19 (C<sub>0</sub>= 25 mg L<sup>-1</sup>, H<sub>2</sub>O<sub>2</sub> conc. 0.5 mM, pH 3.5, US power = 8 W cm<sup>-2</sup>)

Fig. 6 (b). The effect of iron sulphate addition on the rate constant

Fig. 7. UV/Visible absorption changes with reaction time (C<sub>0</sub>= 25 mg L<sup>-1</sup>, H<sub>2</sub>O<sub>2</sub> conc. 0.5 mM, FeSO<sub>4</sub> conc. 3 mg L<sup>-1</sup>, pH 3.5, US power = 8 W cm<sup>-2</sup>)

Fig. 8 (a). The effect of initial dye concentration on the decolorization of RB 19 (H<sub>2</sub>O<sub>2</sub> conc. 0.5 mM, FeSO<sub>4</sub> conc. 3 mg L<sup>-1</sup>, pH 3.5, US power = 8 W cm<sup>-2</sup>)

Fig. 8 (b). The effect of initial dye concentration on the rate constant

Fig. 8 (c). First order kinetic plot of RB 19 degradation by combined ultrasound and Fenton process at different dye concentrations (H<sub>2</sub>O<sub>2</sub> conc. 0.5 mM, FeSO<sub>4</sub> conc. 3 mg L<sup>-1</sup>, pH 3.5, US power = 8 W cm<sup>-2</sup>)

Fig. 9. The effect of different gases on the decolorization of RB 19 ( $C_{0=}$  25 mg L<sup>-1</sup>, H<sub>2</sub>O<sub>2</sub> conc. 0.5 mM, FeSO<sub>4</sub> conc. 3 mg L<sup>-1</sup>, pH 3.5, US power =8 W cm<sup>-2</sup>)

Fig. 10 (a). The effect of ultrasonic powers on the decolorization of RB 19 ( $C_{0=}$  25 mg L<sup>-1</sup>, H<sub>2</sub>O<sub>2</sub> conc. 0.5 mM, FeSO<sub>4</sub> conc. 3 mg L<sup>-1</sup>, pH 3.5)

Fig. 10 (b). The effect of ultrasonic power settings on the rate constant

ACCEPTED MANUSCRIPT

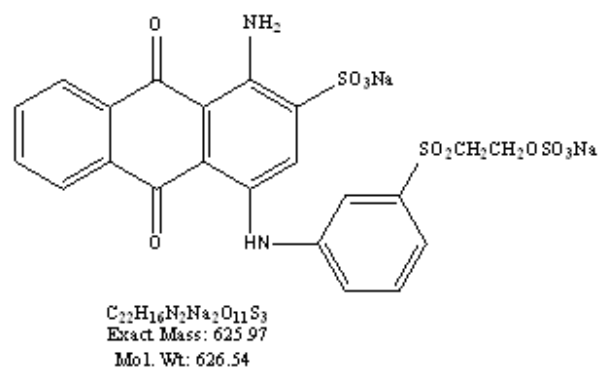


Fig. 1.

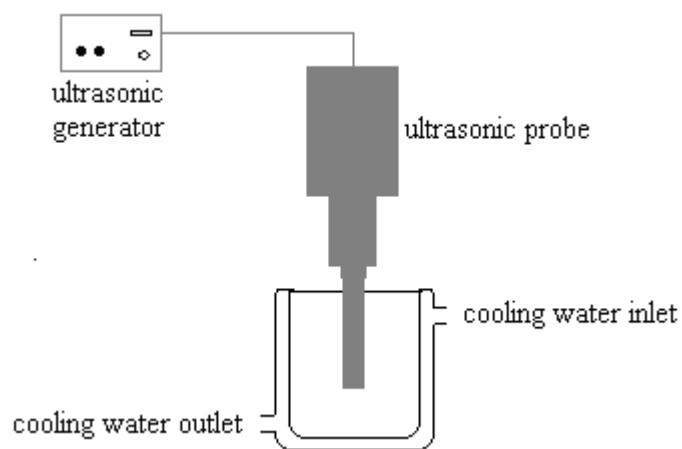


Fig. 2.



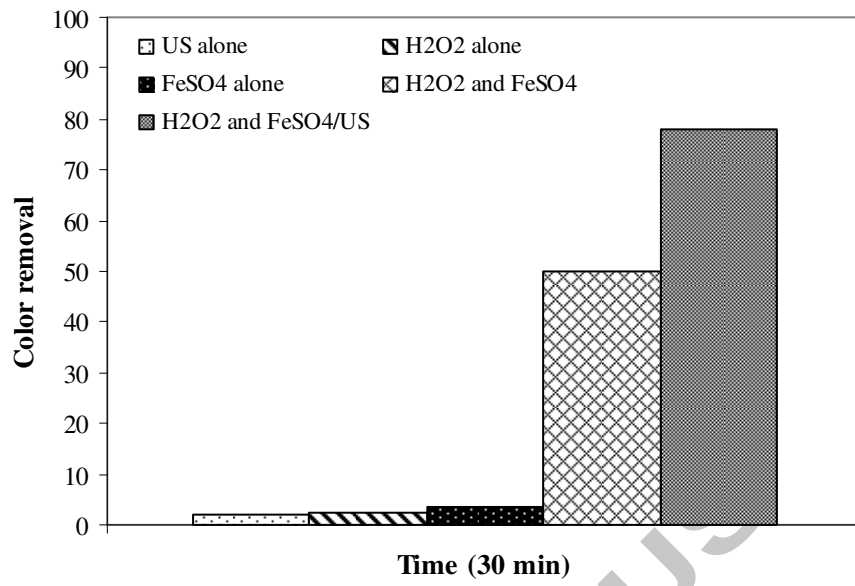


Fig. 3

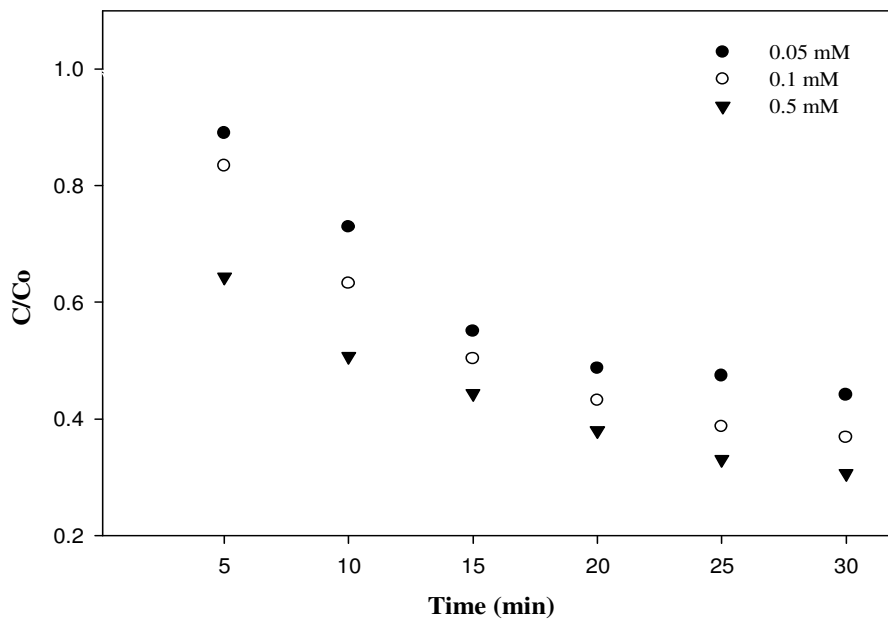


Fig. 4 (a).

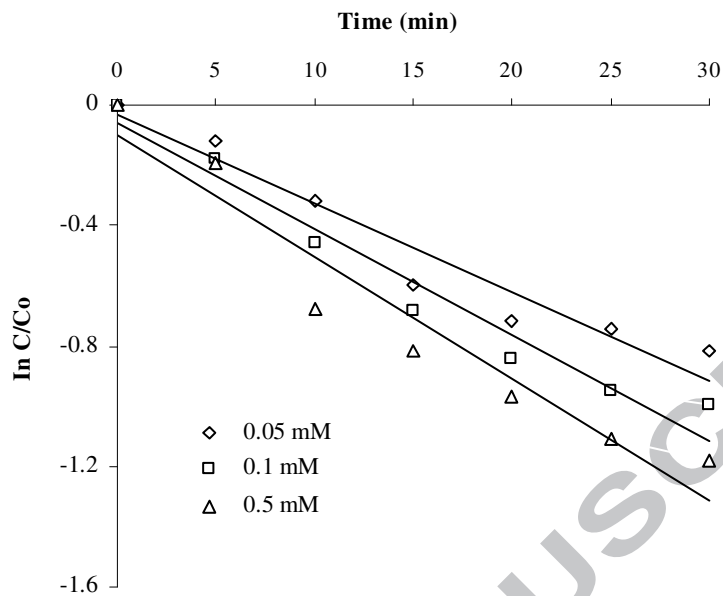


Fig. 4 (b).

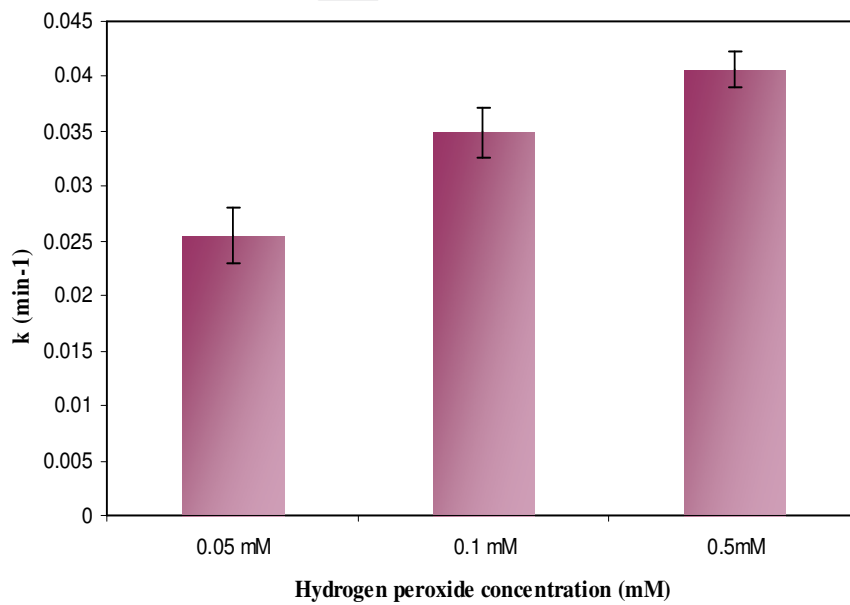


Fig. 4 (c).

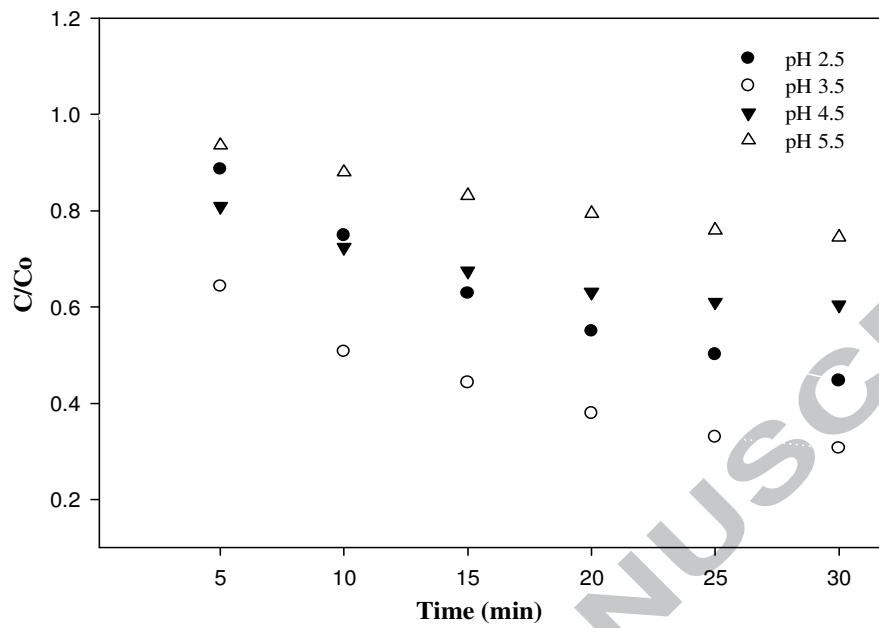


Fig. 5 (a).

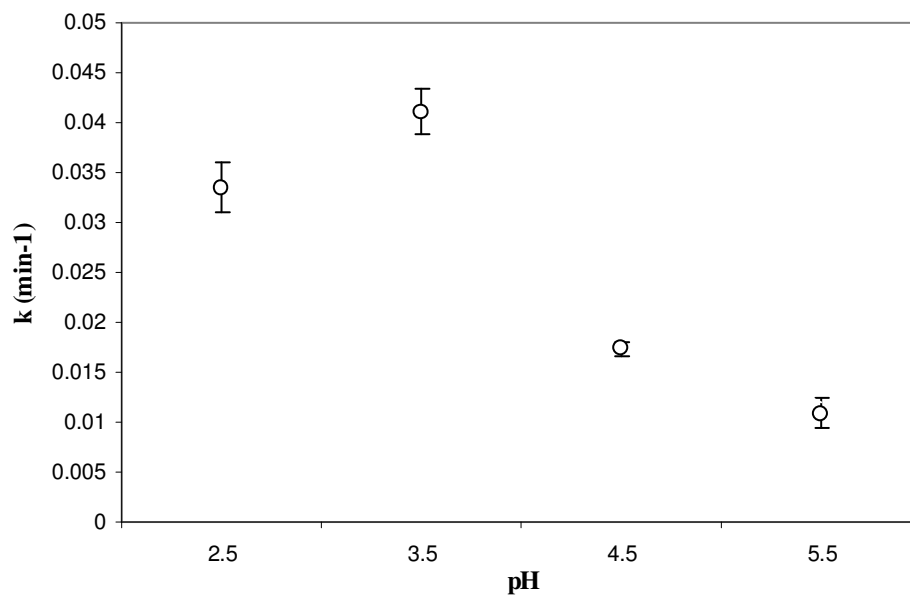


Fig. 5 (b).

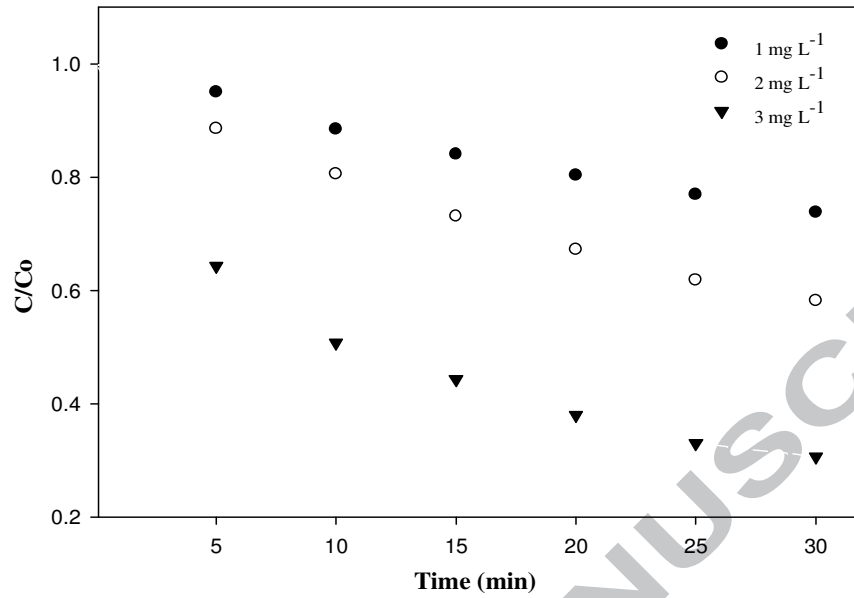


Fig. 6 (a).

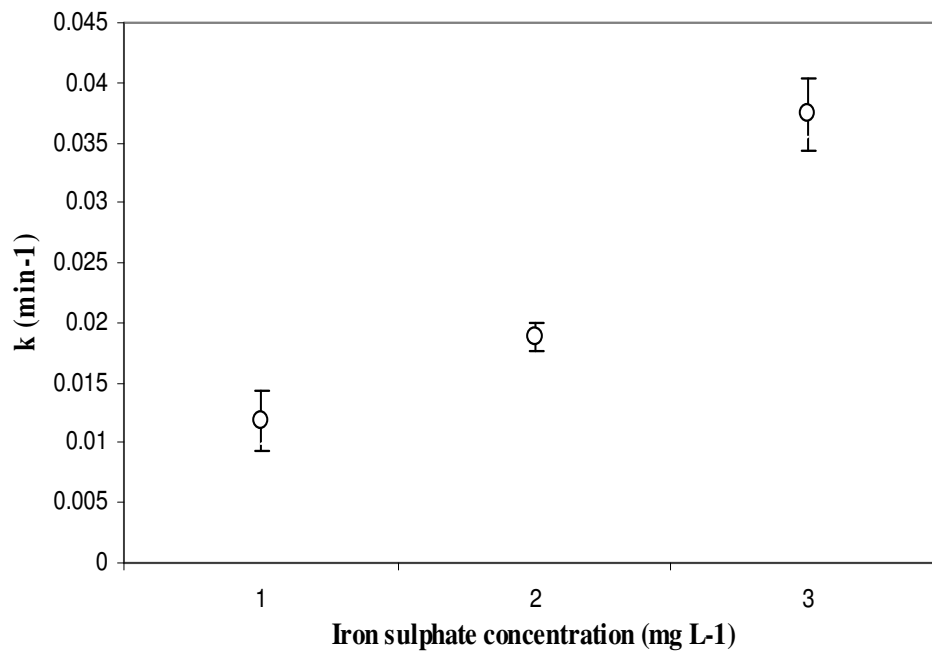


Fig. 6 (b).

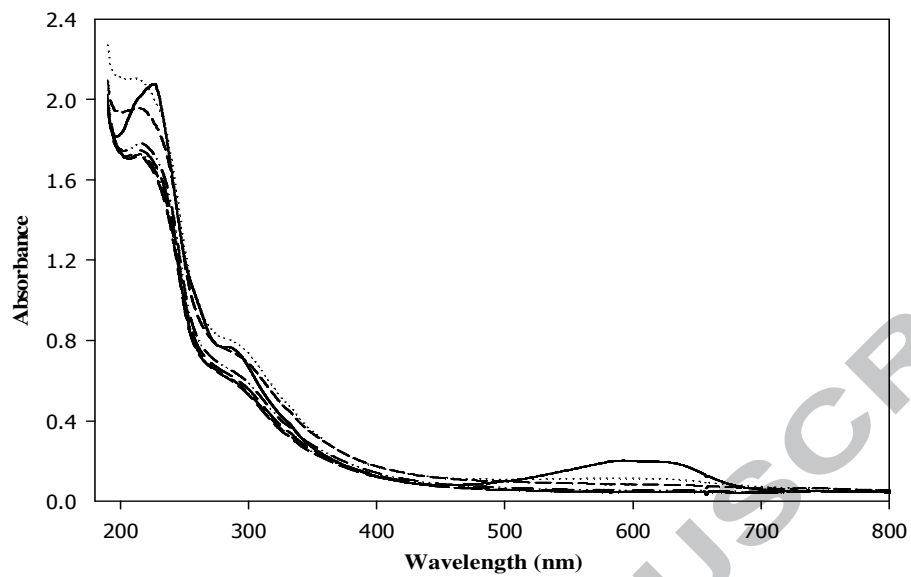


Fig. 7.

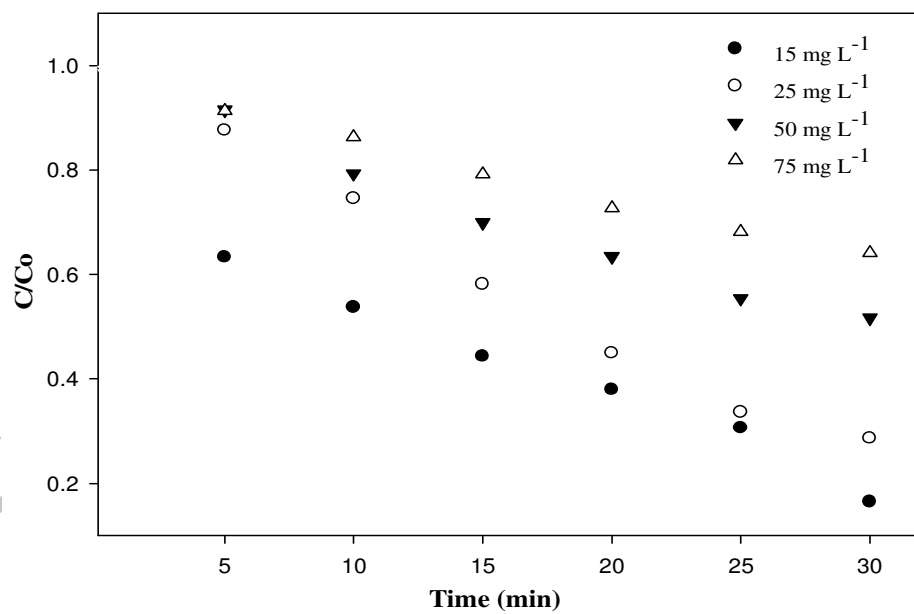


Fig. 8 (a).

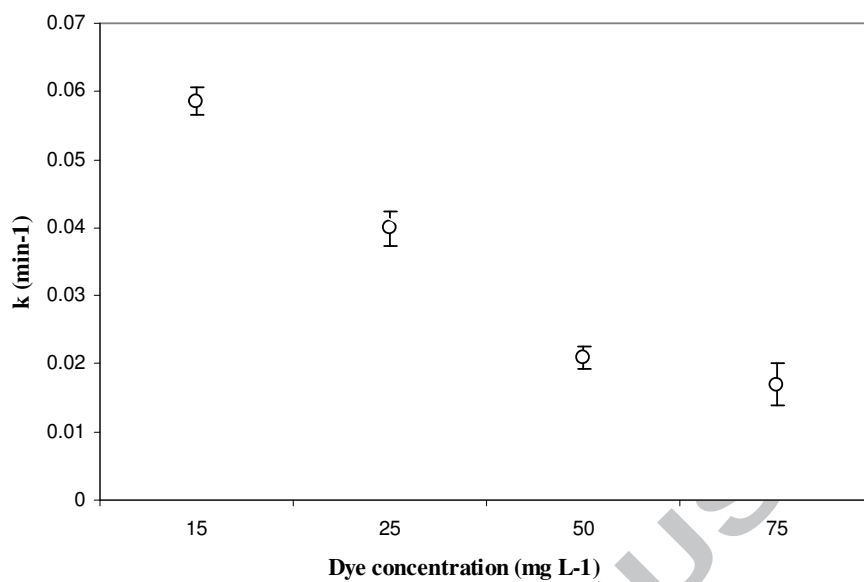


Fig. 8 (b).

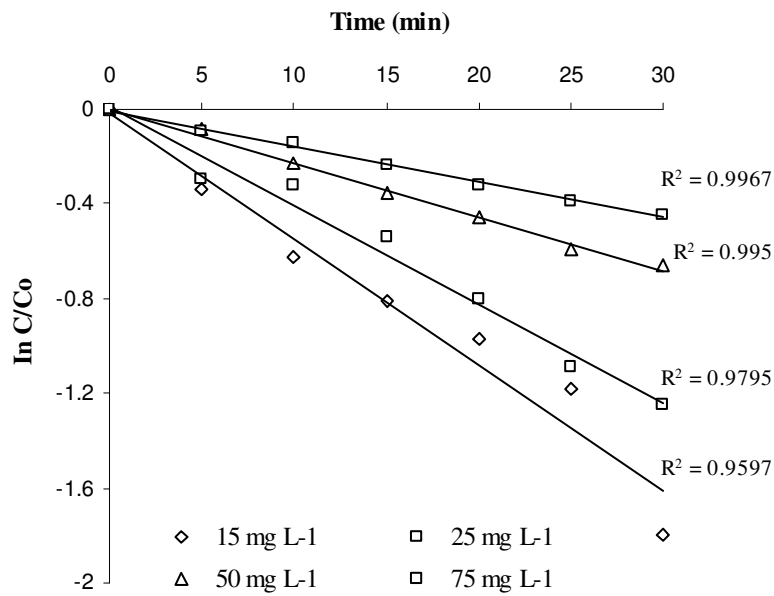


Fig. 8 (c).

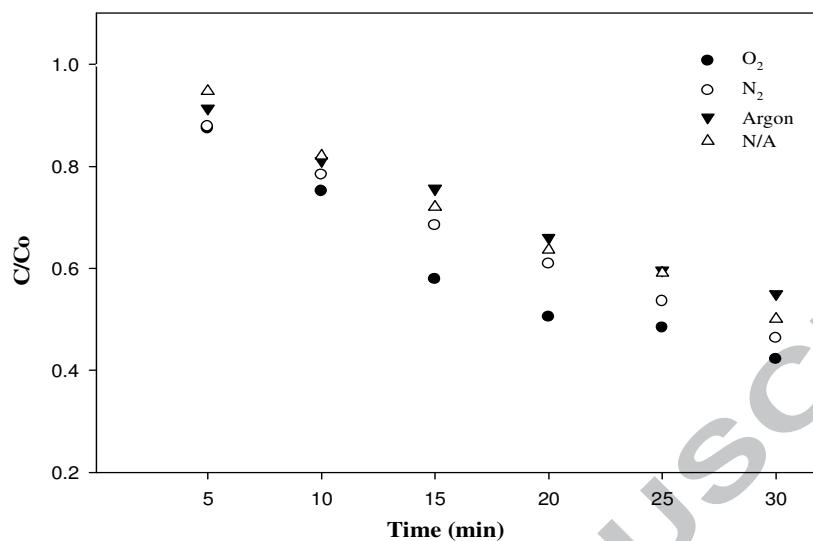


Fig. 9.

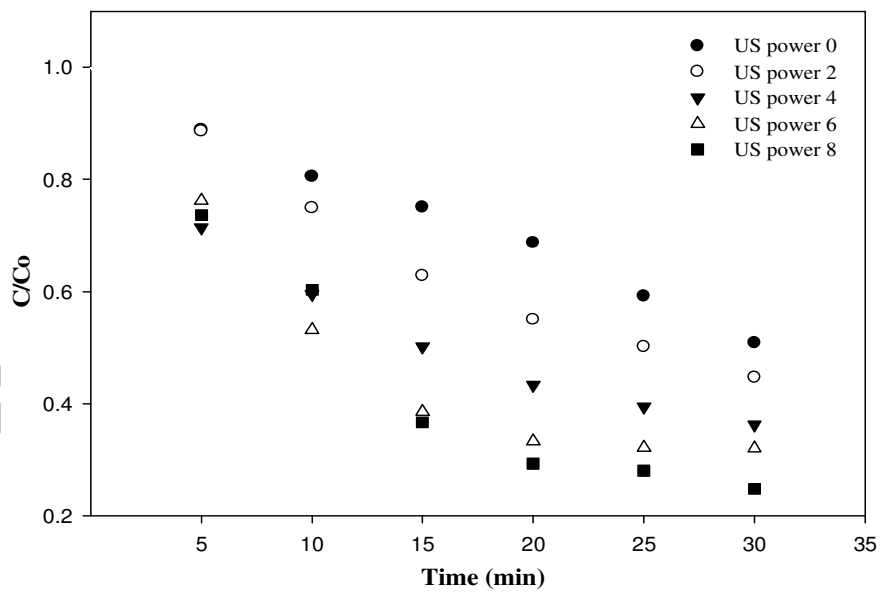


Fig. 10 (a).

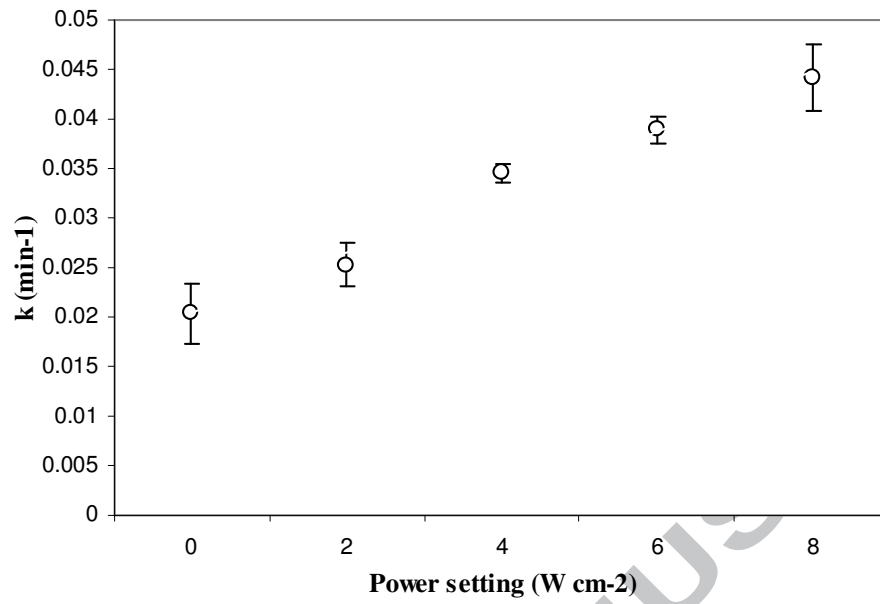


Fig. 10 (b).



Table.1: Comparison of rate constant ( $\text{min}^{-1}$ ) values between US power settings ( $\text{W cm}^{-2}$ ) and Fricke dosimetry

Ultrasonic power settings ( $\text{W cm}^{-2}$ )	$k \text{ min}^{-1}$ (US)	$k \text{ min}^{-1}$ (US) - $k \text{ min}^{-1}$ (no US)	$k \text{ min}^{-1}$ (Fricke)
0	0.0204	--	--
2	0.0253	0.0041	0.00044
4	0.0345	0.0141	0.00105
6	0.0389	0.0185	0.0018
8	0.0442	0.0238	0.00235